Why the pore geometry model could affect the uniqueness of the PSD in AC characterization

J. P. Toso, V. Cornette, Víctor A. Yelpo, J. C. Alexandre de Oliveira, D. C. S. Azevedo & R. H. López

Adsorption
Journal of the International Adsorption Society

ISSN 0929-5607

Adsorption
DOI 10.1007/s10450-016-9760-6

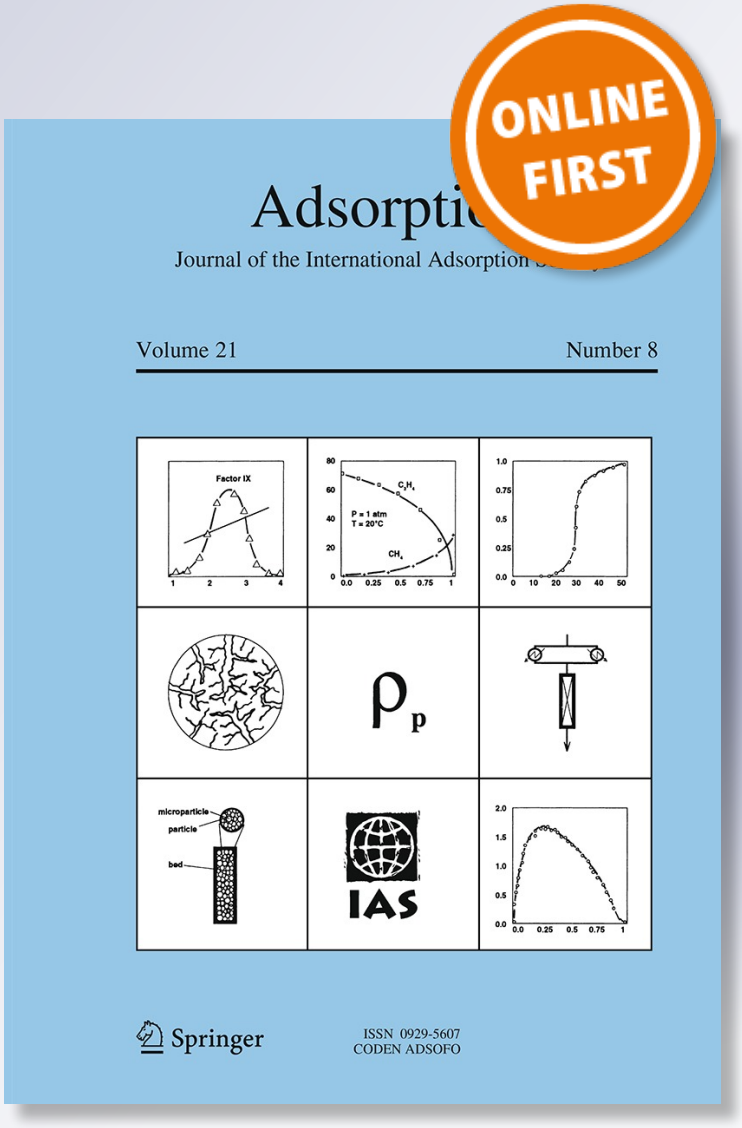

Springer

Adsorption
DOI 10.1007/s10450-016-9760-6

Why the pore geometry model could affect the uniqueness of the PSD in AC characterization

J. P. Toso[1] · V. Cornette[1] · Víctor A. Yelpo[1] · J. C. Alexandre de Oliveira[2] · D. C. S. Azevedo[2] · R. H. López[1]

Received: 11 September 2015 / Revised: 27 December 2015 / Accepted: 4 January 2016

Abstract In this paper we discuss why the pore geometry can affect the unicity of the pore size distribution (PSD) of a given activated carbon (AC) sample, when different probe gases are used in adsorption measures. In order to characterize the solid sample we used grand canonical Monte Carlo simulation and the independent pore model with slit or triangular pore geometry, focusing our analysis on the possibility of representing the adsorptive processes of a triangular pore of defined size by means of a combination of slit pores of different sizes. This representation is tested on experimental adsorption data of N_2 (77 K) on AC samples and acceptable results were obtained. Finally, we have performed a theoretical test, which consisted of analyzing a virtual porous solid with this approach and different probe gases (N_2 at 77 K and CO_2 at 273 K), showing that the differences between the pore representations can cause differences between the solid representations for the adsorptive properties, for these different gases. The analysis presented here can be extended to other pore geometries and other adsorbates, and provide arguments to further explain results presented in our previous paper, which refers to cases when different adsorbates yield different PSDs for a given sample and the same pore geometry model.

✉ R. H. López
rlopez@unsl.edu.ar

[1] Departamento de Física, Instituto de Física Aplicada "Giorgio Zgrablich", CONICET-Universidad Nacional de San Luis, Av. Ej. de Los Andes 950, 5700 San Luis, Argentina

[2] Grupo de Pesquisa em Separações por Adsorção (GPSA), Departamento de Engenharia Química, Universidade Federal do Ceará, Fortaleza, Ceará, Brazil

Keywords AC characterization · PSD · GCMC · Pore geometry

1 Introduction

Activated carbons (AC) are considered as suitable materials for a number of separation and storage processes, due to their low cost and the nearly unlimited possibilities of tuning textural and surface properties (Mash and Rodríguez-Reinoso 2006; Rouquerol et al. 1999). The structure of AC is still at the present a matter of discussion, given the complexity arising from a disordered arrangement of not well defined building blocks (Mash and Rodríguez-Reinoso 2006; Thomson and Gubbins 2000). Nevertheless, a quite simple model, the so-called independent pore model (Lastoskie et al. 1993), has been extensively used for decades to represent such structure. This model considers the porous material as a collection of independent pores of different sizes, all having the same geometry. The slit model is usually assumed for the characterization of ACs and has been extensively used in determining their PSD however, it is reasonable to assume that, at least in part of the material, carbon plates may accommodate in such a way as to form pores with other geometries (Azevedo et al. 2010; Bojan and Steele 1998; Davies and Seaton 1998; Jagiello et al. 2011; De Oliveira et al. 2011). By taking into account such model, it is possible to follow different methodologies (Davies et al. 1999; Gusev et al. 1997; Jagiello 1994; Lueking et al. 2009; Sweatman and Quirke 2001) to characterize the pore size distribution (PSD) of a given AC from experimental adsorption data of a probe molecule. In order to analyze a solid sample, such methodologies require an experimental adsorption isotherm $N_{\mathrm{exp}}^{GAS}(P_i, T)$, which represents the amount of adsorbed gas

Published online: 11 January 2016

on the solid at pressure P_i ($i = 1, \ldots, n$) and temperature T. The next step consists in fitting the experimental isotherm with a model isotherm $N_{\mathrm{mod}}^{GAS}(P_i, T)$, so that a minimum residue R, is defined by (Davies et al. 1999):

$$R \equiv \sum_{i=1}^{n} \left[N_{\mathrm{exp}}^{GAS}(P_i, T) - N_{\mathrm{mod}}^{GAS}(P_i, T) \right]^2 \quad (1)$$

where

$$N_{\mathrm{mod}}^{GAS}(P_i, T) \equiv \sum_{j=1}^{m} f_j^{geom\_GAS} A_{i,j}^{geom\_GAS} \quad (2)$$

and

$$A_{i,j}^{geom\_GAS} \cong \rho_{i,j}^{geom\_GAS}(H_j^*, P_i, T)\, \delta H_j \quad (i = 1, \ldots, n) \quad (3)$$

From Eq. (2), the model isotherm is defined as a linear combination of m ($j = 1, \ldots, m$) curves $\rho_{i,j}^{geom\_GAS}(H_j^*, P_i, T)$, each of which corresponds to the adsorption isotherm of a pore of a given geometry with average pore diameter H_j^*. The minimization of residue R (Eq. 1) is accomplished with suitable values of $f_j^{geo\_GAS}$ ($j = 1, \ldots, m$) by means of a non-negative least square regression (NNLSQ) algorithm. The values $f_j^{geo\_GAS}$ thus obtained define the PSD assigned by the model to the sample, according to a given geometry.

It is important to note that the PSD, as obtained from Eqs. (1)–(3), is affected by the hypotheses taken into account by the model (pore shape and independence, surface heterogeneities, how the adsorbate molecule is represented, gas–solid and gas–gas interaction potentials, etc.).Therefore, the solid matrix defined by the obtained PSD is hardly a realistic representation of the irregular AC sample matrix, but instead it defines an effective porous material whose adsorptive properties are similar to those of the actual solid (Lastoskie et al. 1993; Lueking et al. 2009). A direct consequence of fitting an experimental isotherm with Eqs. (1)–(3) is that two different kernels (for instance of distinct geometries) may be able to represent the same experimental isotherm, giving rise to different PSDs. Within the framework of the independent pore model, this means that a given solid sample may have more than one model matrix that represents its adsorption properties.

As we mentioned above, the issue of AC modeling with pore geometries other than the slit pore model has been addressed several times in the literature. For instance, Davies and Seaton (1998) discuss the case of square and rectangular pore geometries. They show that a monopore isotherm belonging to either one of these geometries may be expressed as a linear combination of model isotherms from a slit-geometry kernel. Due to this "equivalence" and to its simplicity, these authors conclude that the slit geometry should be the most adequate one for represent the porous matrix of a given AC sample. Nevertheless, Davies and Seaton also argue that, due to the fact that different pore geometries may represent the same experimental isotherm, one should exercise caution when trying to calculate characteristic textural parameters, such as the average pore size. Another aspect concerning the use of Eqs. (1)–(3) to assess the PSD of a solid sample is the concern as to whether the PSD*s* obtained with different probe molecules (for the same model) could be equal or different, which has been addressed by several authors including our own recent work. (Gauden et al. 2004; Jagiello and Thommes 2004; Quirke and Tennison 1996; Ravikovitch et al. 2000; Soares Maia et al. 2011).

In this paper, we have used the independent pore model (Eqs. 1–3) for a number of cases of pure slit or pure triangular pore geometries. Following the reasoning of Davies and Seaton (1998), we have developed an approximation which attempts to express the adsorption isotherm of a triangular-shaped monopore as a combination of isotherms from the slit kernel. With this, it was possible to represent the adsorption isotherm, corresponding to a triangular pore matrix, by using a slit pore matrix. This representation is tested on experimental adsorption data of N_2 (77 K) on AC samples, and acceptable results were obtained.

Finally, we have performed a theoretical test, which consisted of applying the obtained representation to the adsorption process (for different probe gases on a virtual porous solid). The results from the test provide arguments to further explain results presented in a previous paper (Toso et al. 2013), which refers to cases when different adsorbates yield different PSD*s* for the same sample and the same pore geometry model. Therefore, the central objetive of the present paper is to explain why the choice of a given assigned pore geometry in a model of independent pores may cause that different probe molecules on the same porous solid sample lead to different PSD*s*.

2 Theoretical aspects

In the following, we have considered N_2 (T = 77 K) and CO_2 (T = 273 K) as adsorbates, until atmospheric pressure. As pore geometry models, we have considered separately the slit and triangular pore geometries (Fig. 1). Pore walls are considered as homogeneous graphite planes (infinite for slit geometry and truncated for triangular geometry) with gas–solid interactions described by the 10-4-3 Steele potential and the Bojan–Steele equation respectively (Bojan and Steele 1998). Both adsorbates were represented

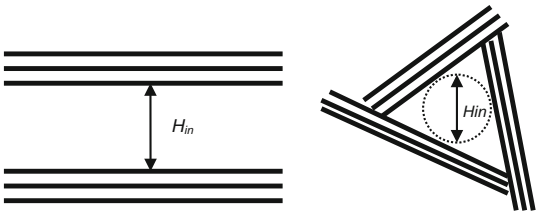

Fig. 1 Slit (*left*) and triangular (*right*) geometry pore showing how the size H_{in} is defined

as one-center molecules. In the confined space of real pores, especially pores that accommodate three layers or less, the pseudo-sphere model describes the adsorption badly, however in a virtual porous solid sample treating CO_2 (or N_2) as a single LJ molecule or as a multi-site potential model will not affect our results qualitatively (with respect to the PSD). For each of the two adsorbates, by means of grand canonical Monte Carlo (GCMC) (Frenkel and Smit 1991; Nicholson and Parsonage 1982) simulations the respective kernels $\rho_{i,j}^{slit\_GAS}$ and $\rho_{i,j}^{trian\_GAS}$ (Eq. 3) were calculated using Lennard–Jones gas–gas and gas–solid parameters, as reported in Ravikovitch et al. (2000).

In this paper, the terms *rPSD_slit* and *rPSD_trian* denote the PSD which results from the fit of an experimental or pseudoexperimental (from virtual solid) isotherm with Eqs. (1)–(3), for the slit and triangular pore geometries, respectively. Likewise, the terms *sPSD_slit* and *sPSD_trian* denote a *source PSD*, which is arbitrarily generated to define a given virtual solid composed of either slit or triangular shaped pores, respectively.

3 Results and discussion

Starting from the idea of Davies and Seaton (1998), it should be possible to represent the adsorptive properties of a triangular monopore with a combination of slit pores. To this end, we presented the following equation:

$$A_{i,j}^{trian\_GAS} \cong \sum_{k=1}^{m} g_{k,j}^{GAS} A_{i,k}^{slit\_GAS} \quad (i = 1, \ldots, n) \qquad (4)$$

Equation (4) is an approximate expression (considering a given gas) for the j-th $A_{i,j}^{trian\_GAS}$ ($i = 1, \ldots, n$) curve, which is written as a function of kernel $A_{i,k}^{slit\_GAS}$ ($j = 1, \ldots, m$). For each j value, which stands for a given pore diameter of the triangular geometry, coefficients $g_{k,j}^{GAS}$ ($k = 1, \ldots, m$) are obtained from NNLSQ. Because the curves $A_{i,j}^{geom\_GAS}$ are proportional to the isotherms $\rho_{i,j}^{geom\_GAS}$ (Eq. 3), it may be stated that Eq. (4) postulates the possibility of representing the adsorptive processes of a triangular pore of defined size by means of a combination of slit pores of different sizes.

Application of Eq. (4) for three different triangular monopores is depicted in Fig. 2 with N_2 (T = 77 K) as adsorbate. It may be observed that a combination of slit pores may fit the isotherm of a triangular monopore when the pore size is large enough (Fig. 2b, c). This is not the case of Fig. 2a, where a triangular monopore of 3.8 Å was considered. The lack of agreement between the original isotherm and that obtained from a slit pore kernel is due to the fact that, for very small micropores ($H_{in} \leq 5$ Å), the same gas uptake tends to be reached at much lower pressures for a triangular pore than for a slit pore of the same size. This is also why the *rPSD* from a slit kernel shown in

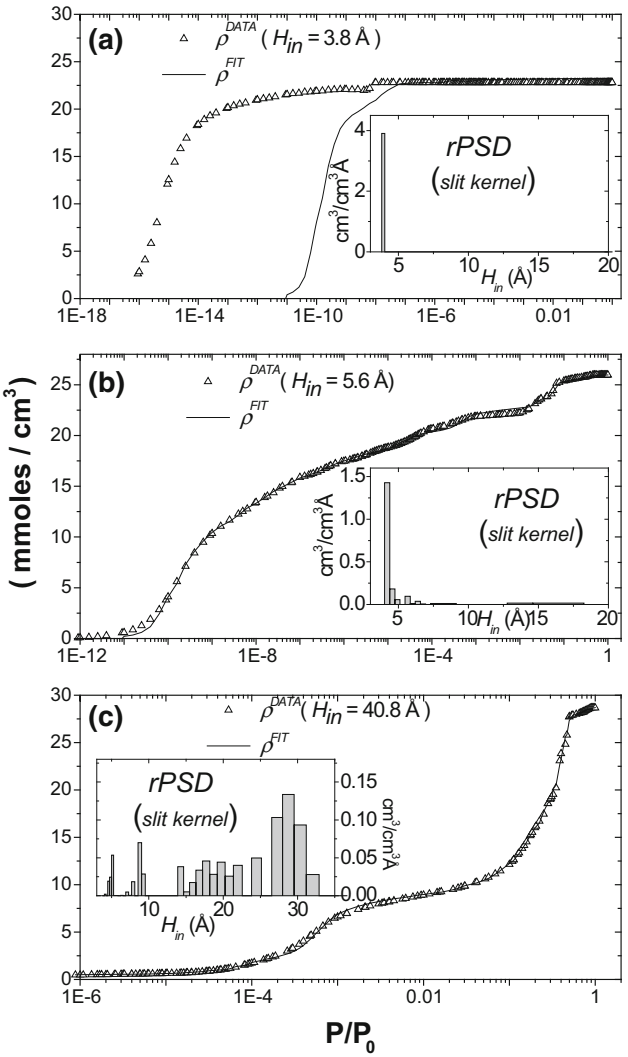

Fig. 2 Application of Eq. (4) to triangular monopore of different diameters (H_{in} = 3.8, 5.6, 40.8 Å): (*open triangle*) triangular monopore adsorption isotherms (N_2 at 77 K) and (*continuous line*) the corresponding slit kernel fitting curve. The *rPSDs* obtained by fitting (slit kernel) are shown in the *inset*

Fig. 2b, c always start from lower diameters than the actual triangular monopore being considered. It is not possible to have smaller slit-shaped pores than the size of the adsorbate, and this is why the *rPSD* shown in Fig. 2a has about a single pore size with the same dimension as the starting triangular monopore. Figure 2b, c shown another aspect [as discussed by Davies and Seaton (1998)] derived from Eq. (4), which has an important consequence as far as modeling is concerned: a sample having a narrow PSD of triangular geometry will correspond to a spread PSD if its isotherm is fit with a slit pore kernel, giving rise to a substantial discrepancy between the sample structure and its "modeled" representation.

By introducing the development of $A_{i,j}^{trian\_GAS}$ (Eq. 4) into the expression of the isotherm $N_{\mathrm{mod}}^{GAS}(P_i,T)$ for the case of a triangular shaped kernel (Eq. 2), the new expression for this isotherm is given by

$$N_{\mathrm{mod}}^{GAS}(P_i,T) \cong \sum_{j=1}^{m}\left[f_j^{trian\_GAS}\sum_{k=1}^{m}A_{i,k}^{slit\_GAS}\,g_{k,j}^{GAS}\right] \tag{5}$$

By exchanging summations in Eq. (5), we find

$$N_{\mathrm{mod}}^{GAS}(P_i,T) \cong \sum_{k=1}^{m} f_k^{slit*\_GAS}\,A_{i,k}^{slit\_GAS} \tag{6}$$

where

$$f_k^{slit*\_GAS} \equiv \sum_{j=1}^{m} f_j^{trian\_GAS}\,g_{k,j}^{GAS} \quad k=1,\ \ldots,\ m \tag{7}$$

The physical meaning of Eq. (6) is similar to that of Eq. (4): while Eq. (4) corresponds to the representation of the adsorptive properties of a single triangular pore as a function of a slit pore kernel, Eq. (6) corresponds to the representation of the adsorptive properties of a triangular pores matrix (whose isotherm is the starting $N_{\mathrm{mod}}^{GAS}(P_i,T)$ given by Eq. (2) by means of a slit pores matrix. As a matter of fact, Eq. (7) should allow to obtain the *PSD_slit* equivalent to a given *PSD_trian*, as far as adsorptive processes are concerned. Such PSD, obtained from the *PSD_trian* and as defined by the coefficients $f_k^{slit*\_GAS}$ (Eq. 7), will be here denoted as *PSD_slit** (i.e. by "*"), in order to distinguish it from the *rPSD_slit* and the *sPSD_slit*. Both Eqs. (6) and (7) will be the core of the remaining discussion in this section.

Table 1 summarizes the residual errors between three class of model isotherms and experimental isotherms for N_2 (T = 77 K) on a set of AC samples synthesized by chemical activation of lignocellulosic precursors. Samples A and B were obtained from peach stones (Soares Maia et al. 2011) whereas samples C and D, from coconut shells (Toso et al. 2011). The first and second rows corresponds to those model isotherms obtained by direct fit to experimental data (Eq. 1) with slit and triangular pore geometry respectively, while the third row correspond to the model isotherm obtained from *PSD_slit** (Eq. 7). According to the *R* values obtained by direct fit (first and second rows), for some samples (A and B), the slit pore geometry is the one that best fits experimental data, whereas for others (C and D) it is the triangular pore geometry which provides a better fit of experimental isotherms. This is an evidence that, even though a kernel of a given geometry may be equivalent to that of another geometry (as shown previously), different geometries will not always be able to fit the same set of experimental data with the same accuracy. With respect to the *R* values obtained from *PSD_slit** (third row), it is observed that Eq. (7) works reasonably in approximating experimental adsorption data of real solids. On the other hand, those *R* values (third row) are closer to the *R* values corresponding to the pore geometry with the worst fit (larger residues), which may be explained as follows: if the triangular pore geometry provides the best fit of experimental data, no other slit geometry would improve such fit and vice versa, so that *PSD_slit** will incorporate the error of the *rPSD* (*rPSD_trian* or *rPSD_slit*) with larger residue.

Table 1 Residues between experimental and model isotherms (N_2 at 77 K) for AC samples obtained by chemical activation of lignocellulosic precursors

$R \equiv \sum_{i=1}^{n}\left[N_{\mathrm{exp}}^{N_2} - N_{\mathrm{mod}}^{N_2}\right]_i^2$

$N_{\mathrm{mod}}^{N_2}$	Sample			
	A	B	C	D
By direct fit: *trian. geom.*	0.33	0.22	14.11	9.70
By direct fit: *slit geom.*	0.71	0.50	9.08	3.58
From *PSD_slit** (Eq. 7)	0.81	0.67	15.25	9.61

Figure 3 shows detailed data for samples B and C, in terms of the PSDs and cumulative volumes, as calculated from the three strategies used for the Table 1. By comparing the *rPSD_slit* with the corresponding *PSD_slit** for both samples, it is clear that both predict similar trends. Additionally, the agreement between *rPSD_slit* and *PSD_slit** is remarkably better for sample B than for sample C, which is directly related to the *R* values shown in Table 1: if *rPSD_trian* fits the experimental data of sample B better than that of sample C, then the "prediction" provided by Eq. (7) will also be better for the former sample than for the latter, because this equation assumes that starting PSD of the sample may be adequately represented by a kernel of triangular geometry. On the other hand, there is an expected discrepancy *rPSD_slit* and

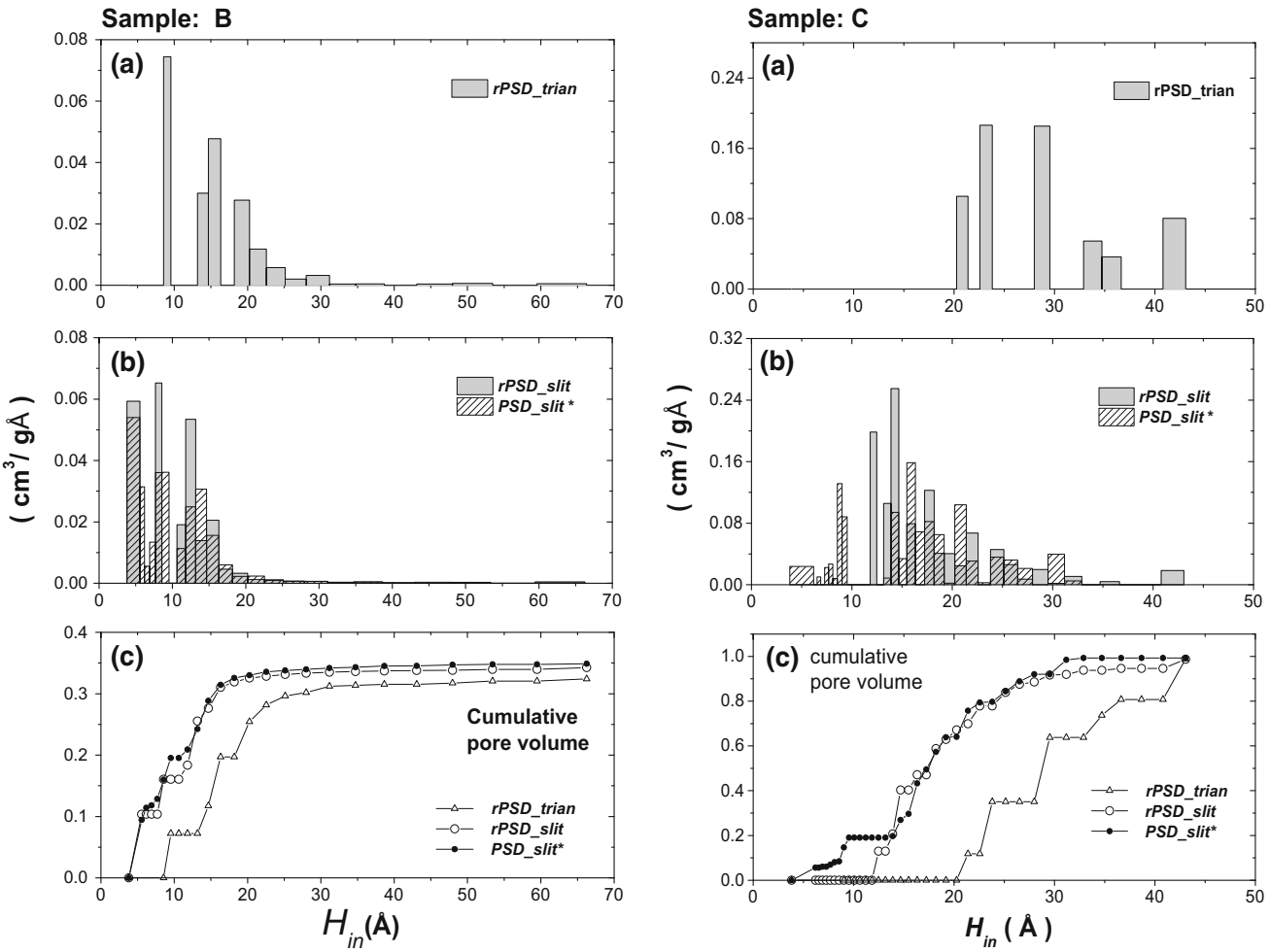

Fig. 3 Application of Eq. (7) to AC samples. The *rPSD_slit* and the *rPSD_trian* are obtained by direct fit from N_2 (T = 77 K) experimental adsorption isotherm of sample B and C (Table 1) and the PSD_*slit** are obtained by Eq. 7. The corresponding cumulative pore volume is compared in the *bottom row*

rPSD_trian for both samples, which agrees with the fact that models that assume different pore geometries will yield different PSD*s* by fitting the same set of experimental data, that is, the same sample.

Figure 4 illustrates the application of Eq. (4) in the case of probe gases N_2 (T = 77 K) and CO_2 (T = 273 K), for different triangular pore size. For each (triangular) pore size H_j^*, the corresponding *rPSD* from slit kernel, is given by the coefficients $f_k^{slit\_GAS}$ where $f_k^{slit\_GAS} = g_{k,j}^{GAS}/\delta H_j$ ($k = 1, \ldots, m$). It is observed that for a given value of diameter H_j^*, the "PSD" profile defined by the coefficients $f_k^{slit\_N2}$ and $f_k^{slit\_CO2}$ ($k = 1, \ldots, m$) differ notoriously. This means that a triangular monopore isotherm $\rho_{i,j}^{trian\_GAS}$ ($i = 1, \ldots, n$) for a given pore diameter may have different kernel slit representations for different adsorbates. This finding is a crucial point in the analysis shown next.

Figure 5 illustrates the application of Eq. (1) through Eq. (3) to a virtual solid, in the same fashion as described in a previous publication (Toso et al. 2013). The porous matrix of such virtual solid consists of a hypothetical and arbitrary distribution of pores of triangular geometry defined by *sPSD_trian*, which is depicted in Fig. 5a. Figure 5b shows the pseudo-experimental isotherms of N_2 and CO_2 for the virtual solid, which were calculated by applying Eq. (2) using the *sPSD_trian* shown in Fig. 5a and the corresponding triangular pore kernels $A_{i,j}^{trian\_N2}$ and $A_{i,j}^{trian\_CO2}$. In turn, Fig. 5c shows the *rPSD_slit* for N_2 and CO_2, as obtained by fit (Eq. 1) with the corresponding slit pore kernels $A_{i,j}^{slit\_N2}$ and $A_{i,j}^{slit\_CO2}$ to the pseudo-experimental isotherms (Fig. 5b). Finally, Fig. 5d compares the curves of cumulative pore volume for the three cases: the hypothetical *sPSD_trian* and the corresponding *rPSD_slit* for N_2 and CO_2. The figures show the expected difference between the "real" PSD of the triangular pores virtual solid (Fig. 5a) that was taken into account and the PSD*s* resulting from the fit of the pseudo-experimental isotherms of

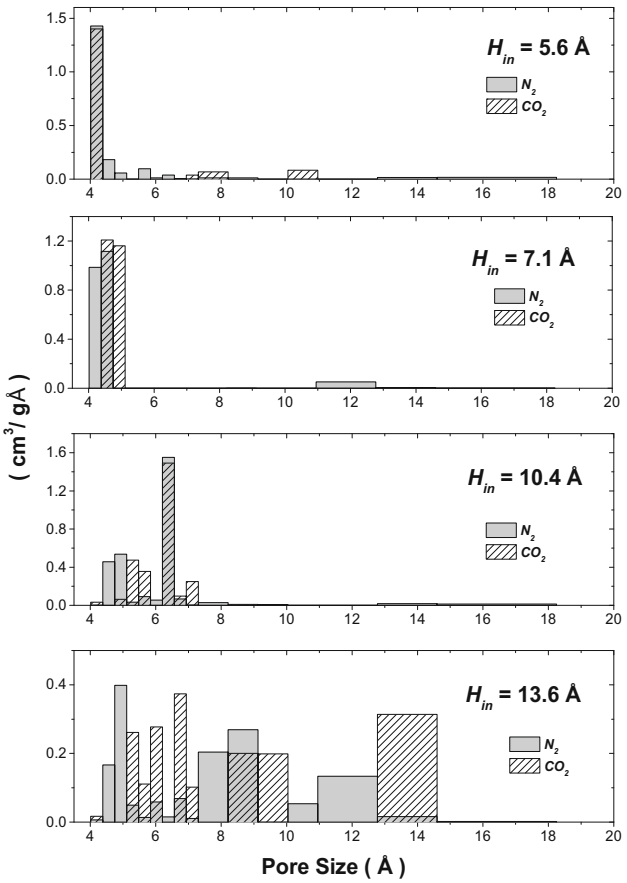

Fig. 4 Application of Eq. (4) to triangular monopore adsorption isotherms of different diameters (H_{in} = 5.6, 7.1, 10.4, 13.6 Å). For each diameter H_{in}, the corresponding *rPSD* (slit kernel) for N_2 at 77 K (*grey*) and for CO_2 at 273 K (*lined*) are compared

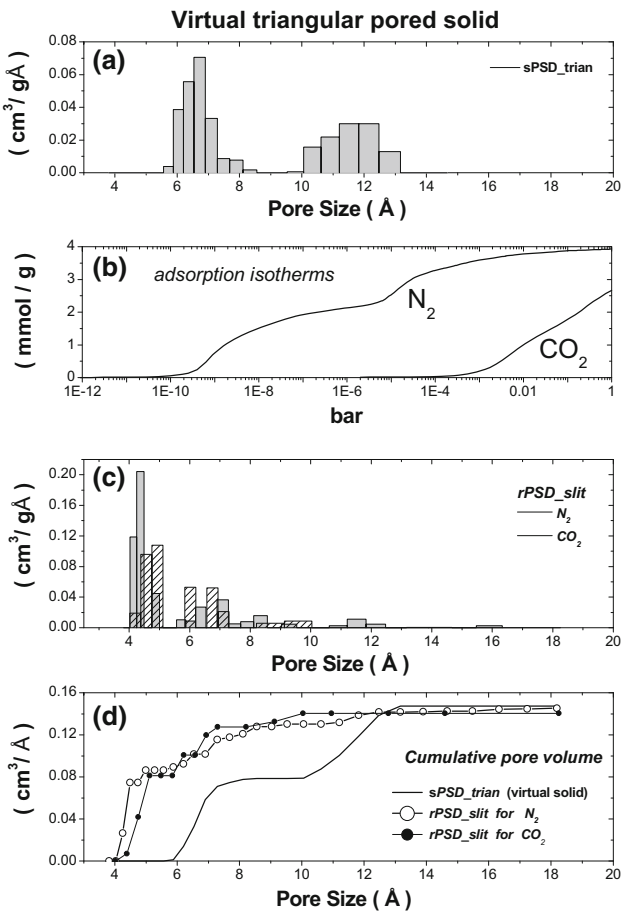

Fig. 5 Theoretical test based on a virtual solid sample with triangular pores. **a** The *sPSD_trian* that defined the solid. **b** The resulting adsorption isotherms for N_2 at 77 K and for CO_2 at 273 K. **c** The *rPSD_slit* obtained by fit the adsorption isotherms with the slit kernel and **d** their cumulative pore volume

either gas assuming slit geometry (Fig. 5c). On the other hand, Fig. 5c shows that the *rPSD_slit* obtained for the same virtual solid with two probe molecules (N_2 and CO_2) show similar trends, but discrepancies are noticeable. Such discrepancy [already reported in Toso et al. (2013)] has an important consequence from the characterization viewpoint and will be discussed more extensively below.

Figure 6 shows the application Eq. (7) to the case of the virtual solid described previously (hypothetical *sPSD_trian* shown in Fig. 5a). For each probe gas, the *rPSD_slit* (see Fig. 5c) is compared with its corresponding *PSD_slit**, which is shown in Fig. 6a, c for N_2 and CO_2 respectively, and a very good agreement is observed in both cases. Note that such agreement is significantly better than that observed for real AC samples (Fig. 3), which can be rationalized by the same argument used to discuss the residues in Table 1: the more the porous matrix resembles a network of independent pores of triangular geometry, the better is the "prediction" of the *rPSD_slit* provided by the *PSD_slit**, and the virtual solid under question fully complies with this condition.

A meaningful result that emerges from Figs. 5 and 6 may be stated as follows. If the *PSD_slit** of a given solid is a good approximation of its respective *rPSD_slit*, then the arguments for discrepancies between the *PSD_slit** for N_2 and CO_2 can be used to explain the discrepancies observed between the *rPSD_slit* of these two gases (see Fig. 4). It has been shown in this Fig. 4, according to the profiles defined by the coefficients $f_k^{slit\_N2}$ and $f_k^{slit\_CO2}$ ($k = 1, \ldots, m$) (considering the same pore size H_j^*) may turn out to be different, which means that the PSD* derived from such coefficients (Eq. 7) may be different for N_2 and CO_2.

4 Conclusions

The problem of the unicity of the PSD of an AC as determined by using different probe gas molecules has been discussed. Through the representation of the

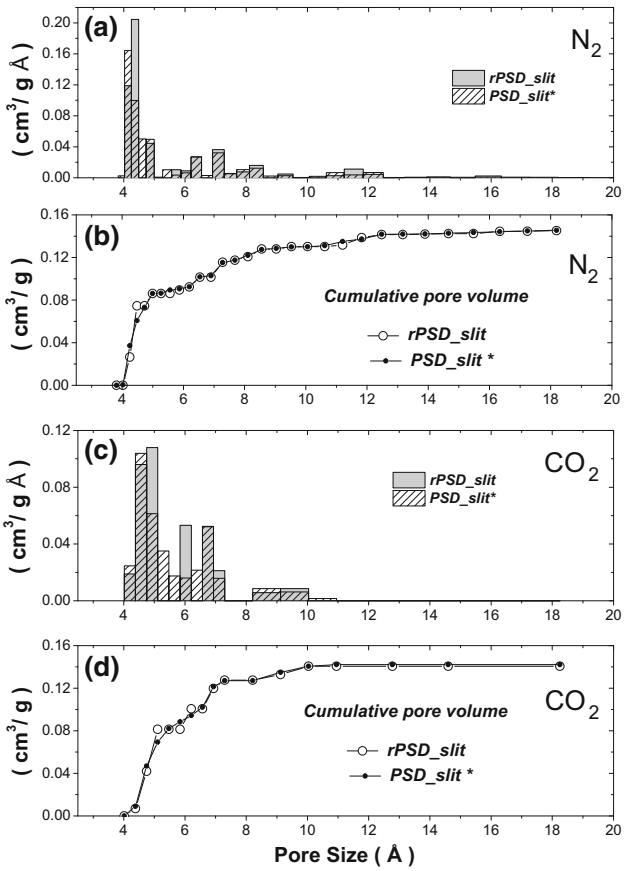

Fig. 6 Application of Eq. (7) to the case of virtual solid described en Fig. 5. **a** The *rPSD_slit* (Fig. 5c) and the corresponding *PSD_slit** obtained by application of Eq. (7) to the *sPSD_trian* (Fig. 5a), for N_2 at 77 K. **b** The cumulative pore volume of the *PSD* show1ed in "**a**". **c** Idem "**a**" for CO_2 at 273 K, **d** Idem "**b**" for the *PSD* shown in "**c**"

adsorptive properties of a single triangular pore as a function of slit pores (kernel), we postulate, in an approximate way, the possibility of representing the adsorptive processes of a triangular defined pore size by means of a combination of slit pores of different sizes. This representation is tested on experimental adsorption data of N_2 (77 K) on AC samples and acceptable results were obtained.

Using this representation a theoretical test in a virtual porous solid (triangular) with different probe gases (N_2 at 77 K and CO_2 at 273 K), which consists in analyzing the adsorption process was developed, showing that, if the representation on a "slit basis" of the adsorptive properties of a triangular pore of a given diameter depends on the probe molecule in question, then the representation on a "slit basis" of the adsorptive properties of a given sample (in this case a triangular pore virtual solid)may has different representations.

The analysis presented here can be extended to other pore geometries and other adsorbates, and provide arguments to further explain results presented in a our previous paper, where we have shown that assuming a pore geometry model different from real geometry of the sample may lead to different PSDs for different probe gases.

Acknowledgments The authors thank CNPq (Brazil) and CONICET (Argentina) for financial support to carry out this research. The numerical works were done using the BACO parallel cluster located at Dpto. de Física - INFAP, Universidad Nacional de San Luis - CONICET, San Luis, Argentina.

References

Azevedo, D.C.S., Rios, R.B., López, R.H., Torres, A.E.B., Cavalcante, C.L., Toso, J.P., Zgrablich, G.: Characterization of PSD of activated carbons by using slit and triangular pore geometries. Appl. Surf. Sci. **256**, 5191–5197 (2010)

Bojan, M.J., Steele, W.A.: Computer simulation in pores with rectangular cross-sections. Carbon N. Y. **36**, 1417–1423 (1998)

Davies, G.M., Seaton, N.A.: The effect of the choice of pore model on the characterization of the internal structure of microporous carbons using pore size distributions. Carbon N. Y. **36**, 1473–1490 (1998)

Davies, G.M., Seaton, N.A., Vassiliadis, V.S.: Calculation of pore size distributions of activated carbons from adsorption isotherms. Langmuir **36**, 8235–8245 (1999)

De Oliveira, J.C.A., López, R.H., Toso, J.P., Lucena, S.M.P., Cavalcante, C.L., Azevedo, D.C.S., Zgrablich, G., Oliveira, J.C.A.: On the influence of heterogeneity of graphene sheets in the determination of the pore size distribution of activated carbons. Adsorption **17**, 845–851 (2011)

Frenkel, D., Smit, D.: Understanding Molecular Simulation. Academic Press, Sidney (1991)

Gauden, P.A., Terzyk, A.P., Rychlicki, G., Kowalczyk, P., Cwiertnia, M.S., Garbacz, J.K.: Estimating the pore size distribution of activated carbons from adsorption data of different adsorbates by various methods. J. Colloid Interface Sci. **273**, 39–63 (2004)

Gusev, V.Y., O'Brien, J.A., Seaton, N.A.: A self-consistent method for characterization of activated carbons using supercritical adsorption and grand canonical Monte Carlo simulations. Langmuir **13**, 2815–2821 (1997)

Jagiello, J.: Stable numerical solution of the adsorption integral equation using splines. Langmuir **10**, 2778–2785 (1994)

Jagiello, J., Kenvin, J., Olivier, J.P., Lupini, A.R., Contescu, C.I.: Using a new finite slit pore model for NLDFT analysis of carbon pore structure. Adsorpt. Sci. Technol. **29**, 769–780 (2011)

Jagiello, J., Thommes, M.: Comparison of DFT characterization methods based on N_2, Ar, CO_2, and H_2 adsorption applied to carbons with various pore size distributions. Carbon N. Y. **42**, 1227–1232 (2004)

Lastoskie, C., Gubbins, K.E., Quirke, N.: Pore size distribution analysis of microporous carbons: a density functional theory approach. J. Phys. Chem. **97**, 4786–4796 (1993)

Lueking, A.D., Kim, H.-Y., Jagiello, J., Bancroft, K., Johnson, J.K., Cole, M.W.: Tests of pore-size distributions deduced from inversion of simulated and real adsorption data. J. Low Temp. Phys. **157**, 410–428 (2009)

Mash, H., Rodríguez-Reinoso, F.: Activated Carbon. Elsevier Ltd, Oxford (2006)

Nicholson, D., Parsonage, N.G.: Computer Simulation and the Statistical Mechanics of Adsorption. Academic Press, London (1982)

Quirke, N., Tennison, S.R.R.: The interpretation of pore size distributions of microporous carbons. Carbon N. Y. **34**, 1281–1286 (1996)

Ravikovitch, P.I., Vishnyakov, A., Russo, R., Neimark, A.V.: Unified approach to pore size characterization of microporous carbonaceous materials from N_2, Ar, and CO_2 adsorption isotherms. Langmuir **16**, 2311–2320 (2000)

Rouquerol, F., Rouquerol, J., Sing, K.: Adsorption by Powders and Porous Solids. Academic Press, San Diego (1999)

Soares Maia, D.A., De Oliveira, J.C.A., Toso, J.P., Sapag, K., López, R.H., Azevedo, D.C.S., Cavalcante, C.L., Zgrablich, G.: Characterization of the PSD of activated carbons from peach stones for separation of combustion gas mixtures. Adsorption **17**, 853–861 (2011)

Sweatman, M.B., Quirke, N.: Modelling gas adsorption in slit-pores using Monte Carlo simulation. Mol. Simul. **27**, 295–321 (2001)

Thomson, K.T., Gubbins, K.E.: Modeling structural morphology of microporous carbons by reverse Monte Carlo. Langmuir **16**, 5761–5773 (2000)

Toso, J.P., López, R.H., De Azevedo, D.C.S., Cavalcante Jr, C.L., Prauchner, M.J., Rodríguez-Reinoso, F., Zgrablich, G.: Evaluation of a mixed geometry model for the characterization of activated carbons. Adsorption **17**, 551–560 (2011)

Toso, J.P., Oliveira, J.C.A., Soares Maia, D.A., Cornette, V., López, R.H., Azevedo, D.C.S., Zgrablich, G.: Effect of the pore geometry in the characterization of the pore size distribution of activated carbons. Adsorption **19**, 601–609 (2013)